Magnetoresistance of Ferromagnetic Nanowires

J-E. Wegrowe, D. Kelly, A. Franck, S. E. Gilbert, and J.-Ph. Ansermet

Institut de Physique Experimentale, Ecole Polytechnique Fédérale de Lausanne CH-1015 Lausanne, Switzerland
(Received 16 March 1998)

Magnetoresistance of single Ni and Co nanowires, of about 60 nm in diameter and 6000 nm in length, was measured at room temperature. The full magnetoresistive hysteresis loops of single Ni nanowires, including the irreversible jump, are understood qualitatively, and major progress has been made towards their quantitative description, on the basis of anisotropic magnetoresistance. In contrast, the magnetoresistive hysteresis loops of single Co nanowires could not be described quantitatively, due to the presence of nucleation processes of domain walls or vortices. [S0031-9007(99)09021-3]

PACS numbers: 72.15.Gd, 75.10.Hk, 75.60.Ej

The ability to engineer magnetic systems on the nanomater scale increasingly produces new physical phenomena and poses challenges to established models of magnetic behavior. The most spectacular of these involves the electrical transport of magnetic nanostructures and the emergence of effects relating to spin-scattering asymmetry which promise a new generation of spin electronic device technology [1]. Exploitation of these effects in device form demands a detailed understanding of both the transport and the magnetization behavior of such nanostructures, at a basic level, yet experimental study is widely frustrated by the general complexity of such systems [2–5]. In this paper we exploit novel preparation methods to present for the first time at coherent study of a single ferromagnetic nanowire whose magnetization reversal better approximates to ideal textbook of magnetic ellipsoid [6]. This simplicity in turn leads us to a better understanding of its magnetization and transport behavior and its explanation in terms of anisotropic magnetoresistance (AMR).

Ni and Co nanowires were produced by electrodeposition in porous membranes. The wires were polycrystalline and 6 μm in length. Their average diameter was 60 nm, and the standard deviation about 20 nm, as measured by transmission electron microscopy [7]. The wires were shown to be magnetically decoupled [8]. The magnetization of one single magnetic nanowire, of the order of 10^{-11} emu (10^{-14} A m^2), cannot be measured with conventional magnetometry, but the magnetization reversal can be detected with near field microscopy [9], electron holography [10], and micro-SQUID [11] techniques. Also the AMR [12], was shown to be adequate for measuring very small magnetization variations. The magnetoresistance of a set of nanowires contacted in parallel in the membrane has been measured previously [13,14]. Here, single nanowires were electrically contacted with a newly developed technique [15], thus making possible the study of magnetization switching in single nanowires by electrical transport measurement.

Anisotropic magnetoresistance is an effect due to the anisotropy of spin-orbit scattering which results in the dependence of the resistance on the angle between the current and the magnetization. According to a commonly accepted view [16,17] the AMR of bulk polycrystalline samples is proportional to $\cos^2 \omega$, where ω is the angle between the current (which is parallel to the wire axis) and the magnetization $M(H)$ (which in turn, is a function of the applied field H). This simple law derives from the high symmetry of the resistivity tensor in bulk materials. However, in the case of magnetic nanostructures, deviations may be expected, due to diffusive scattering at the surface [17]. Neglecting such finite size effects, the magnetoresistive curve $R(H)$ is related to the magnetization $M(H)$ by

$$R(H) = R_0 + (\Delta R)_{\max}\left(\frac{M(H)}{M_s}\right)^2 \qquad (1)$$

when the magnetization is uniform and measured along the wire axis (and hence $M(H) = M_s \cos[\omega(H)]$, where M_s is the saturation magnetization). In Eq. (1), the quantity $(\Delta R)_{\max}/R_0$ defines the AMR ratio.

Our ferromagnetic nanowires are of course the extreme case of an ellipsoidal ferromagnetic particle, and so the nanowire magnetization $M(H)$ may be understood in terms of the physics of magnetic ellipsoid with appropriate modifications. In particular, the magnetic hysteresis loop $M(H)$ of a single monodomain particle is decomposed in a reversible reversal and an irreversible discontinuity, which occurs at the switching field H_{SW}. This jump of the magnetization corresponds to the unstable states responsible for the hysteresis, which are, in turn, peculiar to the magnetization reversal mode. This latter can thus be characterized by measuring the angular dependence of the switching field $H_{\text{SW}}(\theta)$, where θ is the angle between the applied field and the wire axis. The field $H_{\text{SW}}(\theta)$ can be determined experimentally by observing the discontinuity of the magnetoresistive hysteresis. Then, the full magnetoresistive hysteresis loop can be deduced from relation (1) and the micromagnetic model which gives $M(H)$.

The magnetoresistive hysteresis loops of the Ni sample is shown in Fig. 1 for two different angles, 15° and 45°, of the applied field. The resistance R_0 of one wire was about

420 Ω and the AMR ratio 0.8%. $H_{SW}(\theta)$ curves were thus generated for single, isolated Ni nanowires (Fig. 2). The U-shaped curve, which is typical of curling in infinite cylinders without magnetocrystalline anisotropy, had to be corrected for the hump at small angle. This hump can be seen in the data reported by others [9,11]. A recent model of Aharoni shows that the hump occurs when a magnetocrystalline anisotropy parallel to the wire axis is taken into account in the curling rotational mode [18]. The model assumes that the magnetization is uniform before the perturbation into this state. The switching field is the solution of the following system of equations derived from Brown's equation [19] for an ellipsoid of revolution [18]:

$$
\begin{cases}
\dfrac{H}{2\pi M_s}\cos(\theta - \omega) = 2(D_x \sin^2\omega \; - D_z \cos^2\omega) \\[4pt]
\quad - \dfrac{k}{S^2} - \dfrac{K_1}{2\pi M_s^2}(3\cos^2\omega - 1) - 2\dfrac{K_2}{2\pi M_s^2}\sin^2\omega(5\cos^2\omega - 1) \\[8pt]
\dfrac{H}{2\pi M_s}\sin(\theta - \omega) = \left(D_x - D_z + \dfrac{K_1}{4\pi M_s^2} + \dfrac{K_2}{2\pi M_s^2}\sin^2\omega\right)\sin(2\omega)
\end{cases}
\quad , \qquad (2)
$$

where D_x and D_z are the demagnetizing factors of the ellipsoid and K_1 and K_2 are the magnetocrystalline uniaxial anisotropy constants. The parameter S is the reduced radius: $S = r/r_0$. The exchange length is linked to the exchange constant C by the relation $R_0 = \sqrt{C/2M_s^2}$ and is comprised in the range 10 to 20 nm [10]. The radius r was not known exactly. It was in the range of 20 to 40 nm relative to the Gaussian-like distribution of pore diameters [8]. The parameter k is defined in [21]. The parameters D_x, D_z and k are known functions of the aspect ratio. The parameters S and K_1 were used as adjustable parameters (Fig. 2). In our polycrystalline samples, $K1$ is the magnetocrystalline anisotropy constant averaged over the whole cylinder. K_2 was taken to be zero. The uniaxial magnetocrystalline anisotropy K_1 must be about 2×10^5 erg/cm^2 in order to account for the hump at small angles. The bulk magnetocrystalline anisotropy is about $K_1 = 5 \times 10^4$ erg/cm^3. The high value of K_1 found here can be attributed to the strains of Ni grown by electrodeposition. The anisotropy caused by strain can be estimated as induced by magnetostriction. From typical strain values [22], an anisotropy of the order of 10^5 erg/cm^3 can be expected [8]. However, the fit performed with the demagnetizing factors corresponding to the aspect ratio of the cylinder (and $k = 1.079$) over estimates the switching field by about 0.5 kOe. Evidently, an important contribution has been omitted in this description, which facilitates the magnetization reversal. It may come from the surface anisotropy, from a perpendicular magnetocrystalline anisotropy, or more likely, from the structural defects of such polycrystalline Ni wires.
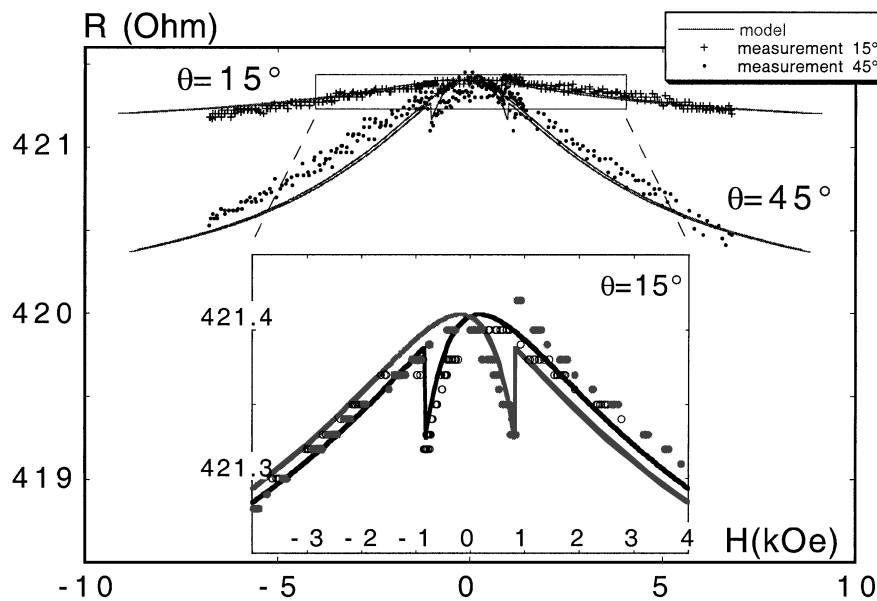
FIG. 1. Ni magnetoresistive hysteresis at 15° and 45°. Bias current 0.3 μA. The continuous lines are predictions based on the curling model of magnetization reversal and the AMR quadratic dependence of the projection of the magnetization in the direction of the current. Inset: Zoom of the magnetoresistive discontinuity at the switching field H_{SW}, for $\theta = 15°$. The points correspond to increasing (full circles) and decreasing (empty circles) field measurements.

This discrepancy could be accounted for in the framework of the present model by supposing that some local defects allow the nucleation of the magnetization in part of the wire only. In this picture, once the longitudinal anisotropy was adjusted to produce the hump at small angles, the shape anisotropy was adjusted by setting the demagnetizing factors to $D_x = 0.426$ and $D_z = 0.148$ ($k = 1.27$), and S to 2.06 (R of about 30 nm). These values correspond to the nucleation of a volume of aspect ratio of about 2:1 [11]. A discrepancy persists above 50°. In the model, large angles correspond to a uniform rotation over the quasitotality of the reversal. A deviation from uniform reversal because of the pinning of the magnetization by surface defects can hence be expected at large angles.

The full Ni magnetoresistance hysteresis loops at 15° and 45° (Fig. 1) were predicted with the parameters of the previous fit to $H_{SW}(\theta)$, and the measured value of the AMR ratio, that is with no adjustable parameter. The following assumptions were made: The stable states have a magnetization direction given by the Stoner-Wohlfarth model of coherent rotation before the jump, and the jump occurs at the field given by the solution of Eq. (2). After the jump, the next stable state was taken to be the magnetization state of the Stoner-Wohlfarth model obtained in a reversed field sweep (inset of Fig. 1). The discrepancies at large angles between the observed values of the switching field and the prediction of the model (Fig. 2) appear also on the whole magnetoresistance hysteresis curves. This shows that the hypothesis of uniform magnetization states before the jump breaks down at larger angles. An alternative explanation for these discrepancies at larger angles could be a deviation from the AMR law (1) due to the finite size effects [17]. Unfortunately, a correction of a few percent to higher order in $\cos^2\omega$ of the magnetoresistance (1) can hardly be observed at small angles, but could account for the weak discrepancy of the AMR curve at 45° (Fig. 1).
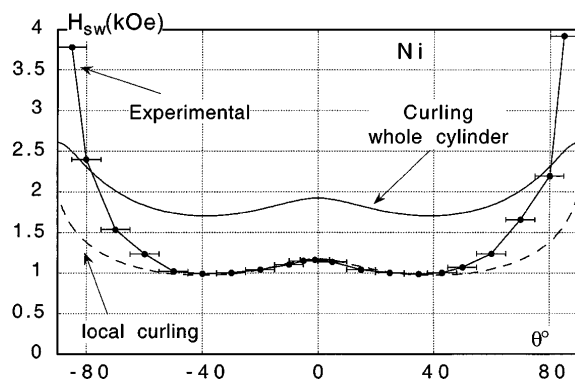
A different picture arises with Co nanowires, where the presence of a domain wall was observed. The comparison of the remanent states at 1° and 85° shows that about $\frac{1}{3}$ of the magnetization is perpendicular to the wire axis (Fig. 3). Neither uniform magnetization reversal nor curling could explain these curves. The jump observed in the inset of Fig. 3 corresponds to the nucleation of a domain wall [23]. An annihilation jump close to the nucleation jump could also be seen at some angles. Note that the $H_{SW}(\theta)$ data measured on single Co nanowires (Fig. 4) were close to the predictions for the switching field obtained by applying the formula of the curling switching field of an infinite cylinder of radius 38 nm without magnetocrystalline anisotropy. However, as long as domain wall states and nucleation and annihilation of domain walls cannot be described micromagnetically, the spin-dependence scattering process responsible of the hysteresis loops in Co nanowires, e.g., domain-wall scattering effects [3,24], cannot be evidenced without further investigation.

In conclusion, our experience with the AMR of nanowires suggests that nanometer scale spin-dependent scattering processes may be studied experimentally only if the underlying micromagnetic configuration is well defined and independently characterized. In the case of Ni nanowires, which displayed the simple micromagnetic configuration characteristic of single domain ellipsoids, the field and angular dependence of the magnetoresistance could be explained quantitatively by the usual anisotropic magnetoresistance model, thereby verifying the quadratic dependence of the resistance on the cosine of the angle between current and magnetization at small applied field angles. From the micromagnetic point of view, the angular dependence of the switching field could be described up to 50° orientation of the applied field using Aharoni's model of curling rotational mode. However, this description applies only when the volume in which the reversal nucleates was assumed to be a "rugby ball" of aspect

FIG. 2. Switching field of Ni nanowires vs angle between wire and field. Dotted line: Values of the switching field of the curling reversal mode in the cylinder 100:1, with magnetocrystalline anisotropy K_1 as adjustable parameter. Solid line: Curling with the previous K_1 and adjustable demagnetizing factors D_z and D_x.
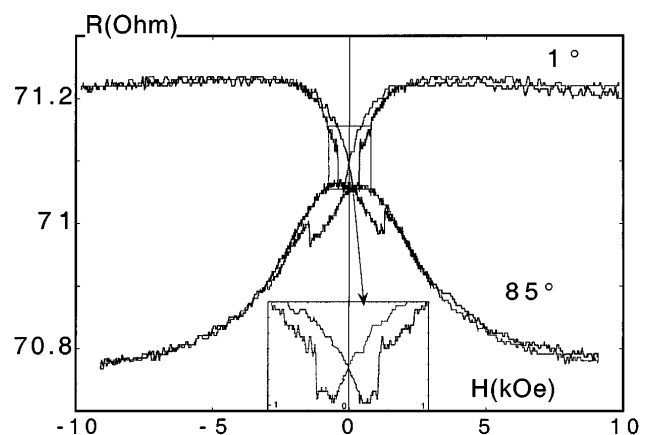
FIG. 3. Magnetoresistive curve of a Co nanowire for longitudinal and transverse applied field. Bias current 1 μA. Inset: Zoom of the magnetoresistive discontinuity for $\theta = 1°$.
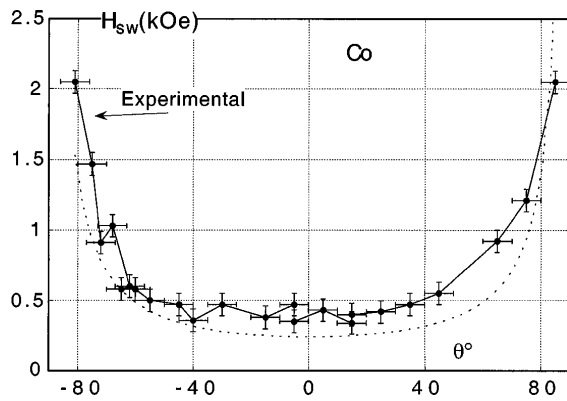
FIG. 4. Switching field of Co nanowires vs angle Dotted line: Curling with anisotropy field $2\pi M_s = 9$ kOe and a diameter of 76 nm, without magnetocrystalline anisotropy.

ratio 1:2, the radius being that of the wire. In this more qualitative picture, a nucleation occurs which involves a volume 50 times smaller than that of the entire wire. The rest of the magnetization follows until the next stable state is reached. A similar scenario was already proposed to account for the small activation volumes measured in identical Ni wires by dynamical measurements [11], and also in the framework of analytical calculation [25] and numerical computations [13,26].

By contrast, the magnetoresistive hysteresis curves of Co nanowires cannot be accounted for quantitatively by simple micromagnetic modeling. The nucleation of domain walls or vortices was already apparent from the data, but the fine details of the micromagnetic configuration were not accessible.

[1] J. Gregg, W. Allen, N. Viart, R. Kirschman, C. Sirisathitkul, J. Ph. Schille, M. Gester, S. Thomson, P. Sparks, V. Da Costa, K. Ounadjela, and M. Skvarla, J. Magn. Magn. Mater. **175**, 1 (1997).

[2] A. O. Adeyeye, J. A. C. Bland, C. Daboo, and D. G. Hsko, Phys. Rev. B **56**, 3265 (1997); A. O. Adeyeye, J. A. C. Bland, and C. Daboo, J. Magn. Magn. Mater. 188, L1 (1998).

[3] U. Ruediger, J. Yu, S. Zhang, A. D. Kent, and S. S. P. Parkin, Phys. Rev. Lett. **80**, 5639 (1998).

[4] Kimin Hong and N. Giordano, J. Phys. Condens. Mater. **10**, L401 (1998); **8**, L.301 (1996).

[5] V. Cros, S-F. Lee, G. Faini, A. Cornette, A. Hamzic, and A. Fert, J. Magn. Magn. Mater. **165**, 512 (1997); Y. Qiang Jia and S. Y. Chou, J. Appl. Phys. **81**, 5461 (1997).

[6] A. Aharoni, *Introduction to the Theory of Ferromagnetism* (Clarendon Press, Oxford, 1996) and references therein.

[7] I. Chlebny, B. Doudin, and J-Ph Ansermet, Nanostruct. Mater. **2**, 637 (1993).

[8] J. Meier, B. Doudin, and J-Ph. Ansermet, J. Appl. Phys. **79**, 6010 (1996).

[9] R. O'Barr and S. Schultz, J. Appl. Phys. **81**, 5458 (1997).

[10] C. Beeli, B. Doudin, J.-Ph. Ansermet, and P. Stadelmann, J. Magn. Magn. Mater. **164**, 77 (1996).

[11] W. Wernsdorfer, K. Hasselbach, A. Benoit, B. Barabara, B. Doudin, J. Meier, and J-Ph Ansermet, Phys. Rev. Lett. **77**, 1873 (1996).

[12] W. Thomson, Proc. R. Soc. (London) **8**, 546 (1857).

[13] R. Ferré, K. Ounadjela, J. M. George, L. Piraux, and S. Dubois, Phys. Rev. B **56**, 14 066 (1997).

[14] J-E. Wegrowe, J. Tuaillon, A. Blondel J. P. Meier, B. Doudin, and J.-Ph. Ansermet, Helv. Phys. Acta **70**, S5 (separanda 1) (1997).

[15] J.-E. Wegrowe, S. E. Gilbert, D. Kelly, B. Doudin, and J.-Ph. Ansermet, IEEE Trans. Magn. **34**, 903 (1998).

[16] T. R. McGuire and R. I. Potter, IEEE Trans. Magn. **11**, 1018 (1975).

[17] Th. G. S. M. Rijks, R. Coehoorn, M. J. M. de Jong, and W. J. M. de Jonge, Phys. Rev. B **51**, 283 (1995).

[18] P. Aharoni, J. Appl. Phys. **82**, 1281 (1997).

[19] W. F. Brown, Jr., Phys. Rev. **105**, 1479 (1957).

[20] E. Koerster and T. C. Arnoldussen, in *Magnetic Recording,* edited by C. D. Mee, and E. D. Daniel (McGraw-Hill, New York, 1987), Vol. 1.

[21] A. Aharoni, J. Appl. Phys. **30**, 70S (1959).

[22] J. B. Kushner, Met. Prog. **81**, 88 (1962).

[23] J-E. Wegrowe, W. Wernsdorfer, A. Sulpice, L. Thomas, B. Barbara, K. Hasselbach, A. Benoit, and D. Mailly, Phys. Rev. B **53**, 6536 (1996).

[24] J. F. Gregg, W. Allen, K. Ounadjela, M. Viret, M. Hehn, S. M. Thompson, and J. M. D. Coey, Phys. Rev. Lett. **77**, 1580 (1996).

[25] H. Suhl, and H. Bertram, J. Appl. Phys. **82**, 6128 (1997).

[26] S. T. Chui and De-Cheng Tian, J. Appl. Phys. **78**, 3965 (1995).